Applied Catalysis B: Environmental 154–155 (2014) 177–182

Contents lists available at ScienceDirect

Applied Catalysis B: Environmental

journal homepage: www.elsevier.com/locate/apcatb

Biomass-derived N-doped carbon and its application in electrocatalysis

Xiao Zhao [a,b], Jianbing Zhu [a,b], Liang Liang [b], Chenyang Li [b], Changpeng Liu [b,**], Jianhui Liao [b], Wei Xing [a,*]

[a] State Key Laboratory of Electroanalytical Chemistry, Changchun Institute of Applied Chemistry, Chinese Academy of Sciences, Changchun, Jilin 130022, PR China

[b] Laboratory of Advanced Power Sources, Changchun Institute of Applied Chemistry, 5625 Renmin Street, Changchun 130022, PR China

ARTICLE INFO

Article history:
Received 17 October 2013
Received in revised form 6 February 2014
Accepted 14 February 2014
Available online 22 February 2014

Keywords:
N-doped carbon
Methanol fuel cell
Chitosan
Sustability
Platinum

ABSTRACT

The economical, green and sustainable preparation of functional carbon materials is of interest for energy storage and conversion technology. Herein, a functional N-doped carbon material (NC) was obtained from green biomass and cheap carbon black. The as-prepared NC enables the formation of highly-dispersed Pt nanocatalyst. Interestingly, compared to a state-of-the-art commercial Pt/C catalyst, the as-prepared Pt/NC catalyst shows a superior electrocatalytic performance with a 1.4-fold improvement in mass activity and a 1.5-fold enhancement in stability for methanol electrooxidation reaction. Thus, the green and earth-abundant biomass materials exhibit the promise in designing and producing functional carbon materials for high-performance electrochemical devices.

1. Introduction

Fuel cells are promising energy conversion devices. Until now, Pt-based metal have been the most effective electrocatalyst for fuel cell reactions. However, the scarcity and high cost of Pt metal limits its large-scale applications [1–7]. As a response, the functional carbon materials as electrocatalyst support display the potential in both boosting performance and reducing cost of electrocatalyst [3,5,8–17]. In particular, nitrogen-doped carbon (NC) has demonstrated the promise in facilitating the dispersion of metal nanoparticles (NPs) and generating the beneficial effects on electrochemical reactions [8,9,12]. However, the current synthesis procedures for NC are usually involved in toxic or expensive precursor such as pyridine [18], aniline [19] pyrrole [5] and porphyrins [8]. This impedes their large-scale and sustainable application to some extent.

To address this point, an intriguing direction is to use economical, green and sustainable biomass materials [20,21]. For instance, the carbon materials were obtained by the hydrothermal carbonization of biomass such as glucose, pine needles and sugar beets [20–22]. Chitosan (CS) as a natural biopolymer has many unique properties such as low-cost, biocompatibility and rich amines making it widely used in bio-fabrication technology [23,24]. However, few reports involve in using CS to synthesize NC although CS shows some attractive properties: (1) CS as biomass material has the economical, green and sustainable merits; (2) CS possesses much higher active nitrogen content than other biomass materials and should be an ideal nitrogen source [23]; (3) CS can uniformly cover substrates, which would promote the uniform incorporation of nitrogen into substrate.

In this report, NC was synthesized using green biomass CS and cheap carbon black. Firstly, the xerogel comprised of CS and carbon black was synthesized by a solvent-evaporation-induced gelation process. Secondly, the xerogel was then heat-treated at 900 °C to obtain NC. Interestingly, the Pt NPs supported onto the as-prepared NC showed a superior electrocatalytic performance for methanol electrooxidation reaction (MOR) compared to a commercial Pt/C and home-made Pt/C electrocatalysts. Thus, this report emphasizes not only the merit of chitosan as nitrogen precursor but also a superior electrocatalytic performance for Pt/NC catalyst.

2. Experimental

2.1. The synthesis of NC and Pt/NC electrocatalyst

Synthesis of NC: 1 g CS (the degree of deacetylation 80% and the molecular weight 50,000 g mol^{-1}) and 1 g Vulcan-XC 72 carbon

* Corresponding author at: 5625 Renmin Street, Changchun 130022, PR China. Tel.: +86 431 85262223; fax: +86 431 85685653.
** Corresponding author.
E-mail addresses: isliuchp@ciac.ac.cn (C. Liu), xingwei@ciac.jl.cn (W. Xing).

http://dx.doi.org/10.1016/j.apcatb.2014.02.027
0926-3373/

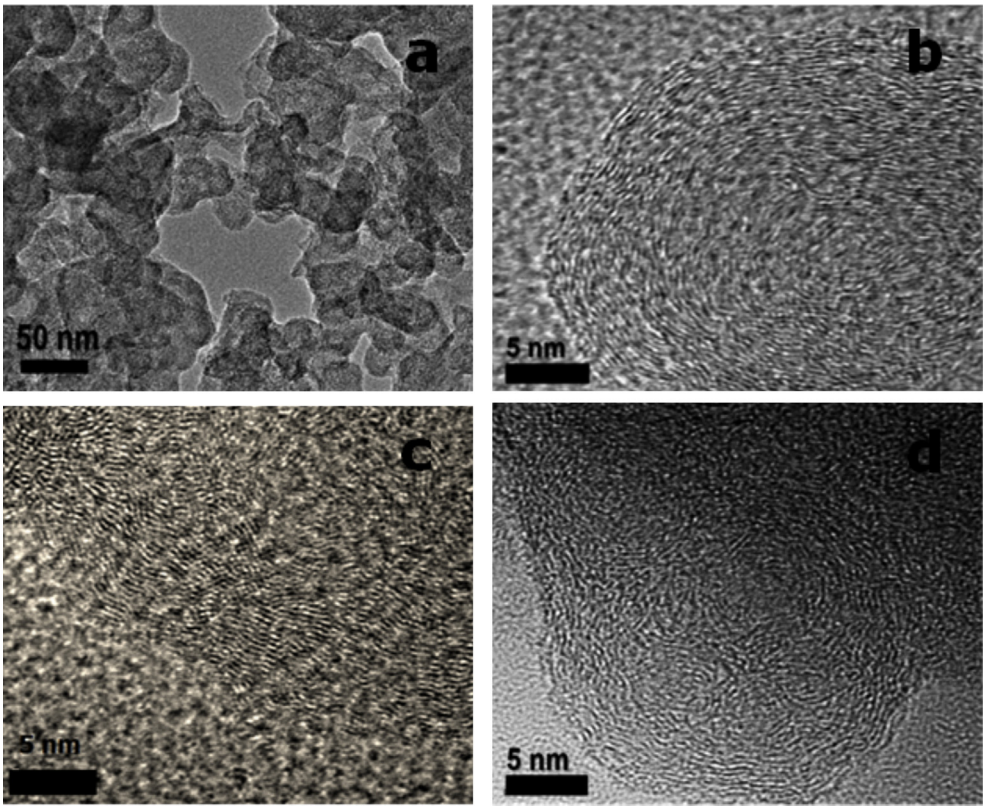

Fig. 1. The represntive TEM image of NC (a) and HRTEM images of NC paritcles (b–d).

black were added into 50 mL acetic acid. The resultant mixture was then extensively stirred and ultrasonically dispersed to form uniform ink. Then, a solvent evaporation-induced gelation process was conducted at 50 °C to obtain the xerogel. The as-prepared xerogel was then heat-treated at 900 °C for 1 h under N_2 atmosphere to obtain the NC.

Synthesis of Pt/NC and Pt/C electrocatalysts: the 20 wt% Pt electrocatalysts were synthesized by a microwave-assisted polyol process in ethylene glycol solution. Briefly, 20 mg NC were ultrasonically dispersed into 20 ml ethylene glycol to form a uniform ink. Then 357 μL H_2PtCl_6 solutions (14 mg mL^{-1}) were added and the pH value of the ink was adjusted to 11 using 0.1 M NaOH solution. Subsequently, the beaker was placed in the center of a microwave oven (800 W) with microwave heating for 90 s. The resulting solution was stirred for 8 h, filtered, washed, and dried in a vacuum oven to obtain Pt/NC. Pt/C was also synthesized using a similar procedure except Vulcan-XC 72 as catalyst supporter. A state-of-the-art commercial Pt/C-JM electrocatalyst (from Johnson Matthey Company, HiSPEC^{TM} 3000) was used as the benchmark electrocatalyst for comparison.

2.2. Physical characterizations

Transmission electron microscopy (TEM) and high resolution TEM (HRTEM) tests were conducted on a TECNAI G2 operating at 200 kV. X-ray photoelectron spectroscopy (XPS) measurements were carried out on a Kratos XSAM-800 spectrometer with an Mg Ka radiation source. X-ray diffraction (XRD) measurements were performed with a PW1700 diffractometer (Philips Co.) using a Cu Ka (λ = 1.5405 Å) radiation source. The obtained XRD patterns were treated with Jade 5.0 software.

2.3. Electrochemical characterizations

Electrochemical measurements were carried out with an EG&G mode 273 potentiostat/galvanostat and a conventional three electrode cell. The catalyst ink was prepared by ultrasonically dispersing the mixture containing 5 mg of catalyst, 950 μL of ethanol and 50 μL of a 5 wt% Nafion solution. Next, a 5 μL droplet of the well-dispersed ink was pipetted onto the pre-cleaned glassy carbon disk (diameter 3 mm) to produce a uniform thin film as working electrode. A Pt foil and a saturated calomel electrode (SCE) were used as the counter and the reference electrodes, respectively. All of the potentials are relative to the SCE electrode, unless otherwise noted. The working electrode was first electrochemically cleaned

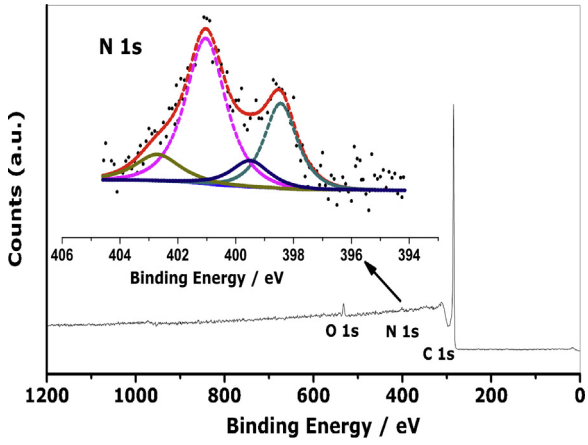

Fig. 2. XPS survey spectra of NC, the inset is high-resolution N 1s spectra.

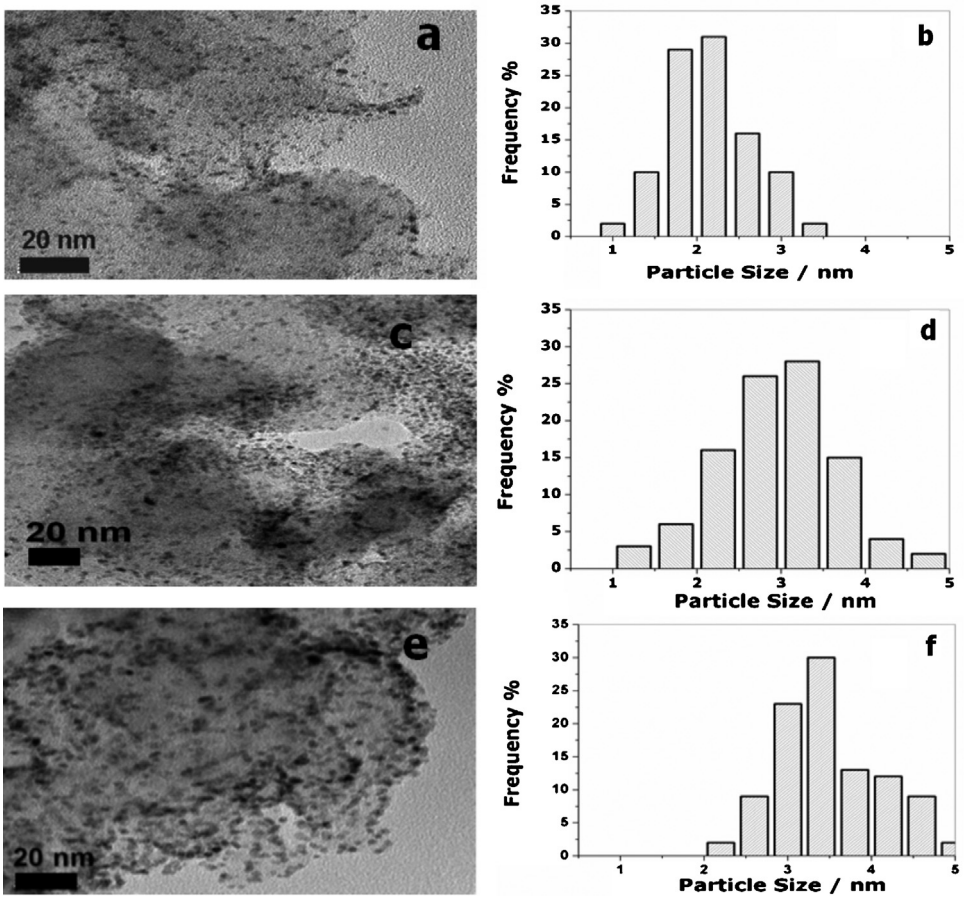

Fig. 3. Representative TEM images and corresponding size distributions of Pt/NC (a and b), Pt/C-JM (c and d) and Pt/C (e and f) electrocatalysts.

via potential cycling from 0.2 V and 1.0 V vs. SCE at 100 mV s^{-1} in a 0.5 M H_2SO_4 solution until a stable response was obtained. To evaluate the activity of the catalysts for MOR, the cyclic voltammetry (CV) experiments were carried out in 0.5 M H_2SO_4 + 1 M CH_3OH solution at a scan rate of 50 mV s^{-1}. To estimate the stability of the catalysts, the chronoamperometric (CA) experiments were performed in the same solution with a potential of 0.5 V. The tolerance to CO poisoning were estimated by the CO stripping test. All electrolyte solutions were de-aerated by high-purity nitrogen for at least 30 min prior to each measurement.

3. Results and discussion

3.1. Physical characterizations

During the solvent-evaporation induced gelation process, biopolymer CS can uniformly form a thin film layer on the surface of carbon black generating a CS shell/carbon black core nanostructure. The sequent pyrolysis enables the carbonation of CS and generates a nitrogen-doped carbon on pristine carbon particle. Fig. 1 shows the representative TEM and HRTEM images of NC with different magnification. The HRTEM images show the carbon particles with (pseudo) shell/core nanostructure surrounded by graphitic carbon layer. The similar nanostructure was also observed in the carbonized polyaniline/carbon black composite [19]. In comparison with polyaniline, the biopolymer CS is more green and economical, and thus guarantees more sustainable application of these NC materials. A closer observation shows some curvature and dislocations presented in the surface layer which may origin from substituted nitrogen atoms leading to the formation of pentagonal defects at the edge and interior of the graphene structure [19].

To demonstrate the successful incorporation of nitrogen into carbon shell, the XPS analysis was conducted. As shown in Fig. 2, the XPS survey patterns for NC displays obvious N1s signal indicating the nitrogen was doped in the carbon layer. The inset in Fig. 2 exhibits the high-resolution data for N 1s which were deconvolved into four components assigned to pyridinic nitrogen at 398.4 eV, pyrrolic N at 399.5 eV, quarternary N at 401.0 eV and oxidized N at 402.7 eV, respectively. The calculated N content is about 3.23 at.%. It is worthy to note that the content of pyridinic and quarternary N dominates an 80 atom% in the whole N functionalities. Generally,

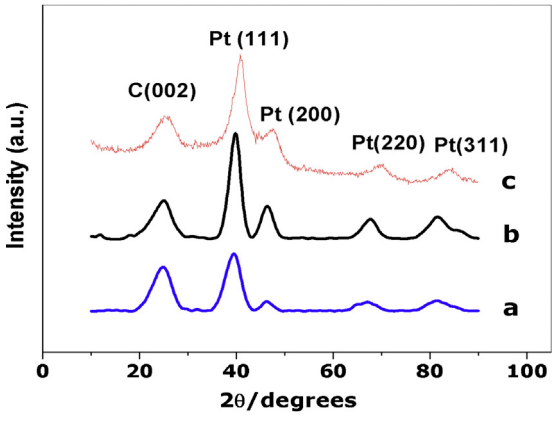

Fig. 4. XRD patterns of Pt/NC (a), Pt/C (b) and Pt/C-JM (c) electrocatalysts.

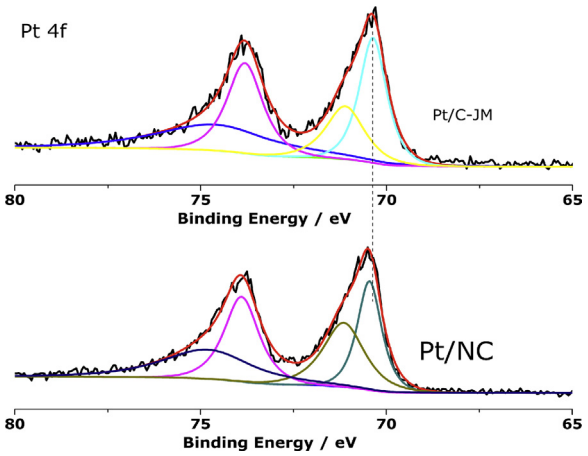

Fig. 5. XPS spectra of Pt 4f region for Pt/C-JM and Pt/NC electrocatalysts.

the rich pyridinic and quaternary nitrogen were correlated with high local electron density of NC materials [25], and can behave as active sites to facilitate Pt reduction and deposition [9].

Fig. 3 presents typical TEM images and the corresponding particle size distribution histograms for Pt/NC, Pt/C-JM and Pt/C electrocatalysts. The particle size distributions were based on 100 particles at random determined from the enlarged images. For Pt/NC electrocatalyst, Pt NPs are homogeneously and densely distributed onto NC support with no evidence of agglomeration. Moreover, Pt/NC catalyst possesses a narrow size distribution and ultrathin particle morphology with a mean size of ca. 2.18 nm. While, Pt/C electrocatalyst exhibits a mean particle size of ca. 3.51 nm with some agglomeration on the un-doped carbon surface. Considering the similar synthesis method, the difference in particles size and distribution between Pt/NC and Pt/C could be ascribed to the N doping as discussed as follows. Pt/C-JM shows highly dispersed Pt NPs with a mean size of 2.98 nm and a slightly agglomeration. It is well known that the surface chemistry of support play a significant role in the nucleation and growth processes during NPs deposition [8,11]. The small Pt NPs and narrow size distributions for Pt/NC catalyst are consistently with the previous reports [8], suggesting that surface chemistry of NC facilitates the formation of highly-dispersed and uniform Pt NPs. Specifically, these nitrogen groups afford the carbon surface with a basic nature and bind strongly to Pt, thereby promoting better dispersion and preventing the agglomeration of Pt NPs [9,26]. In addition, NC features the reducing and electron-rich property, which accelerates the adsorption and reduction of platinum [19]. Herein, the pyrolysis of CS film on carbon black favors the homogeneous incorporation of nitrogen into graphitic carbon layer, which can also be beneficial for the generation of small-sized and highly-dispersed Pt NPs for Pt/NC electrocatalyst as compared with Pt/C electrocatalyst. The crystalline structures for Pt/NC, Pt/C and Pt/C-JM electrocatalysts are shown in Fig. 4. Representative diffraction peaks for Pt (1 1 1), Pt (2 0 0), Pt (2 2 0), and Pt (3 1 1) at are distinctly observed in these XRD patterns. It means that Pt forms a face-centered cubic crystal structure for these three electrocatalysts [11,12,19].

The probe for metal-support interaction is of interest in electrocatalysis as this interaction may remarkably influence the electronic structure and electrocatalysis efficiency of electrocatalyst. XPS as structure-sensitive technique is widely used to investigate oxidation state and electronic structure of catalytic metal. Generally, these factors like morphology, size, composition and nature of the support will show important impact on the electronic structure of catalytic metal. For example, there is a size effect for Pt NPs, that is, the decrease of the particle size is usually accompanied by increasingly positive binding energy shifts [27]. Herein, the comparison of XPS spectra was applied between Pt/NC and Pt/C-JM electrocatalysts due to their close size of Pt NPs. Similar consideration is also applicable for the comparison of methanol electrooxidation and CO electrooxidation [28–30]. Fig. 5 shows the XPS spectra of Pt 4f for Pt/NC and Pt/C-JM electrocatalysts. The Pt 4f signals for both electrocatalysts were deconvolved into two pairs of doublets which can be attributed to metallic Pt (ca. 70.5 eV and 73.9 eV) and Pt(II) in PtO or $Pt(OH)_2$ species (ca. 71.3 eV and 74.8 eV). Interestingly, the binding energies (BEs) of Pt NPs on the NC support slightly shifted to high BEs direction. The up-shifted BEs of Pt 4f for Pt/NC catalyst may be ascribed to the so-called metal-support interaction due to the N doping [9].

3.2. Electrochemical performances of the electrocatalysts

The electrocatalytic performance of these electrocatalysts was evaluated using MOR as a model reaction. Fig. 6a shows the stable CV curves for MOR in a 1 M methanol + 0.5 M H_2SO_4 solution. The Pt/NC electrocatalyst possesses the best electrocatalytic activity for MOR evidenced by the highest anodic peak current density among the three catalysts. The stable anodic peak current density in the forward scan for Pt/NC catalyst is 395 mA mg_{Pt}^{-1} which is ca. 1.6 and 1.4 times higher than Pt/C (252 mA mg_{Pt}^{-1}) and Pt/C-JM (277 mA mg_{Pt}^{-1}), respectively. Interestingly, the Pt/NC electrode also shows higher activity than other Pt/N-doped carbon materials at similar testing condition, for example, Pt/CN (297 mA mg_{Pt}^{-1})

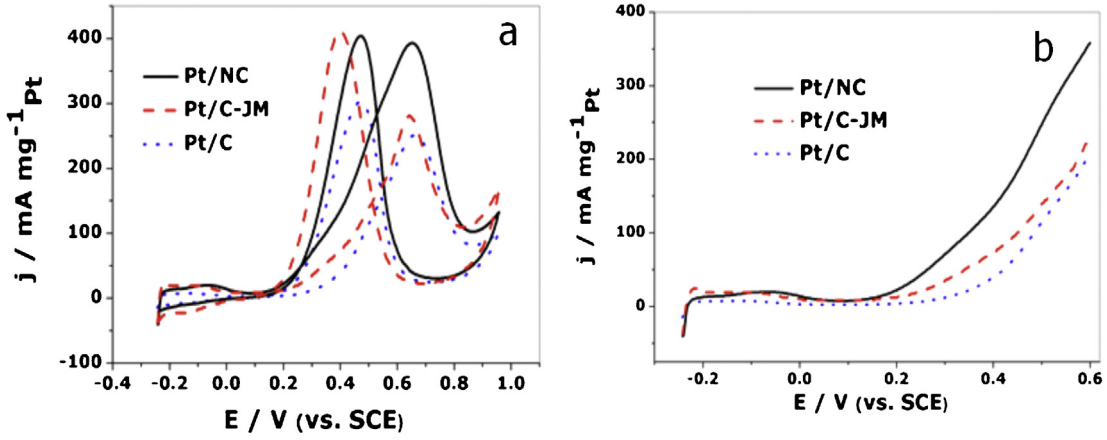

Fig. 6. Mass activity of Pt/NC, Pt/C and Pt/C-JM electrocatalysts for MOR based on CV tests (a) and the enlarged anodic scan curves (b).

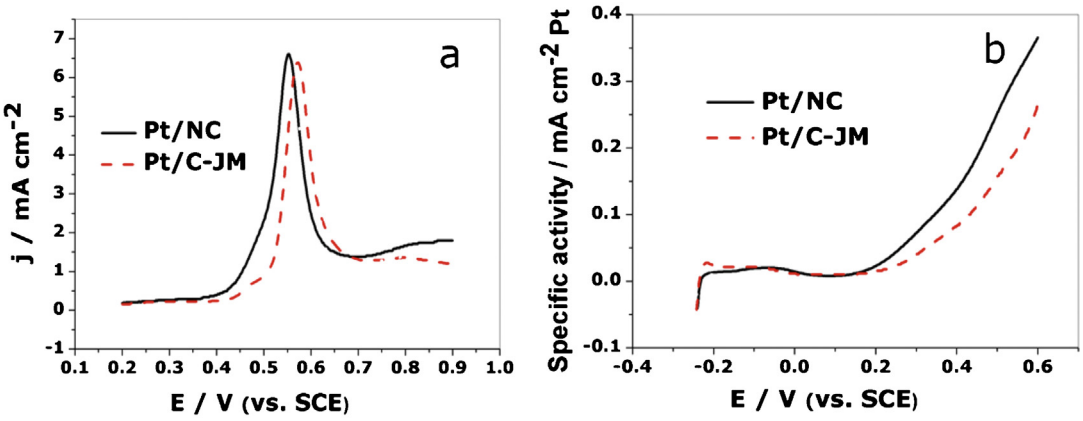

Fig. 7. CO_{ads} stripping curves (a) and area specific activity (b) for Pt/NC and Pt/C-JM electrocatalysts.

obtained by carbonizing polypyrrole nanospheres [5] and Pt/N-doped carbon shells (ca. 275 mA mg_{Pt}^{-1}) synthesized by pyrolysis of polyaniline nanospheres [31]. These results solidly support that the biomass CS can be used as a practical precursor of NC material compared to other toxic and expensive precursors. More importantly, in the technically concerned potential zone, Pt/NC catalyst also shows the consistently improved activity. From the enlarged anodic scan curves in Fig. 6b, Pt/NC electrocatalyst shows an onset potential approximately at 0.157 V vs. SCE which is much lower than Pt/C and Pt/C-JM. The negatively-shifted onset potential and higher current density at low potential zone well attest the improved electrocatalysis efficiency for Pt/NC electrocatalyst.

Fig. 7a shows the CO_{ads} stripping patterns which were used to evaluate the CO_{ads} tolerance and electrochemical surface area (ESA) of electrocatalysts. From the CO_{ads} stripping curves, Pt/NC catalyst shows the lower onset potential for CO oxidation at 0.384 V vs. SCE which is lower than Pt/C-JM (0.430 V vs. SCE). This result indicates the facile removal of CO_{ads} and thus the potentially improved tolerance to CO poisoning for Pt/NC catalyst in MOR. ESA of electrocatalyst is calculated assuming that the coulombic charge required for the oxidation of the CO monolayer was 420 $\mu C\,cm^{-2}$. The ESA for Pt/NC and Pt/C-JM are 98.1 and 88.7 $m^2\,g_{Pt}^{-1}$, respectively. This improved available ESA for Pt/NC can be related to the smaller-sized and well-dispersed Pt NPs and partially account for the improved Pt-based mass activity. Further, it is interesting to investigate the ESA-based intrinsic activity. The intrinsic activities of these electrocatalysts were obtained by normalizing electrode current with Pt ESA. The corresponding curves are shown in Fig. 7b. In the low potential region, an enhanced activity for Pt/NC is observed compared to Pt/C-JM. Therefore, it is safe to conclude that the activity of Pt/NC for MOR is intrinsically enhanced compared to Pt/C-JM.

The stability was further evaluated by CA tests. Fig. 8a shows the CA curves for these electrocatalysts at 0.5 V vs. SCE. Consistent with the CV results, Pt/NC shows a higher initial and stable current density than Pt/C and Pt/C-JM. Considering the difference in the initial current of these electrocatalysts, the current density was normalized by the initial current to obtain the decay rate. The obtained curves are shown in Fig. 8b. The decay rate for Pt/NC catalyst is approximately 36.8% h^{-1} which is much lower than that for the Pt/C-JM (51.6% h^{-1}) and Pt/C (67.0% h^{-1}). Clearly, Pt/NC catalyst shows the superior stability. This result reveals that the NC support provides a unique stabilization effect for the supported Pt NPs during MOR. In combination with the CV results, it can be concluded that Pt/NC displays an enhanced electrocatalytic performance toward MOR compared to a common Pt/C and a commercial Pt/C-JM.

It is well known that MOR on Pt metal comprises of two key reaction steps: the initial methanol dehydrogenation and the sequential oxidation of poisoning intermediates, typical CO_{ads} species. In low potential zone, the rate of methanol dehydrogenation controls the reaction dynamics, whereas in high potential zone, the oxidative removal of poisoning intermediates became the rate-determining step. Based on these consideration, the electronic effect (or ligand effect) and bifunctional mechanism were believed to both effectively facilitate the methanol dehydrogenation and/or inhibit the CO_{ads} poisoning during MOR [1,2]. For the enhanced activity of

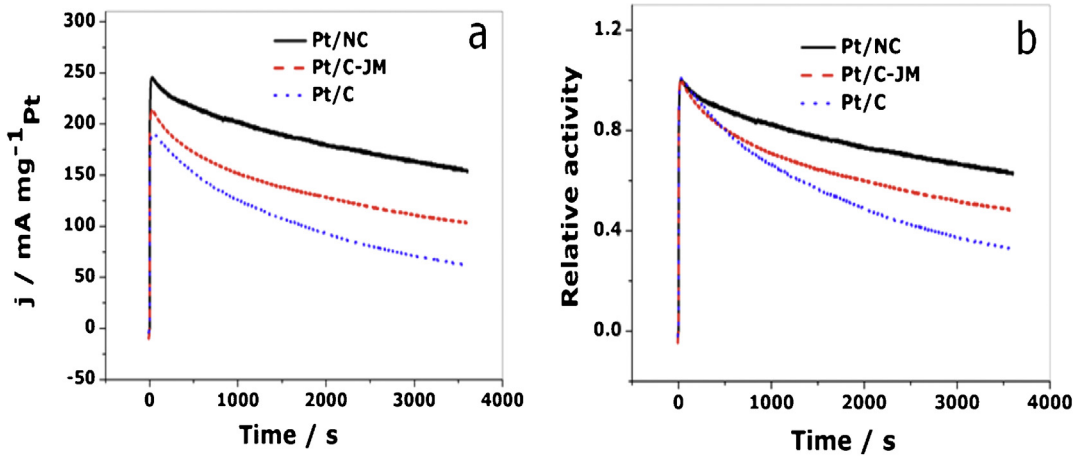

Fig. 8. The stability and relative stability of Pt/NC, Pt/C and Pt/C-JM electrocatalysts based on CA tests at 0.5 V vs. SCE.

Pt/NC for MOR, some clues can be obtained from the physical and electrochemical characterizations. From the XPS analysis of Pt 4f, nitrogen doping seems to modify the electronic structure of the overlying Pt NPs generating the so-called metal-support interaction. According to the works of Norskov and Hammer [32,33], the positive shift in BE of Pt 4f can be correlated with their down-shift d-band center vs. the Fermi level indicating a decrease in the bond strength of adsorbates onto metal surface. The Pt/NC catalyst with a lower d-band center could bind the CO-like intermediate less strongly and thus improve the overall kinetics of MOR. This can be evinced by the facile CO removal, negatively-shifted onset potential of MOR and enhanced intrinsic activity. In addition, recent report indicates that the intrinsic incorporation of nitrogen in the graphitic plane would generate oxophilic C–N defects which are beneficial for activating water to generate OH_{ads} at a lower potential [8]. The active –OH groups would favor the oxidation of CO_{ads} via the bifunctional mechanism in the lower potential zone. The accumulated CO-like species during CA test can degrade the activity of Pt due to the decreased active sites. The enhanced removal of CO-like species will mitigate the degradation of Pt/NC electrocatalyst to some extent and result in the better stability than Pt/C-JM and Pt/C electrocatalysts. Combining these considerations, Pt/NC electrocatalyst indeed show the promising application in direct methanol fuel cells.

4. Conclusions

Pt NPs supported on NC show a high dispersion and exhibit the enhanced activity for MOR compared to a commercial Pt/C electrocatalyst. The nitrogen groups promote the dispersion of Pt NPs and generate a beneficially electrocatalytic effect for overlying Pt NPs. Compared to other nitrogen-doped carbon materials, using biomass CS as nitrogen sources possesses the unique advantages with respect to its eco-friendly, low-cost and sustainable characters. Thus, the green and earth-abundant biomass materials exhibit the promising in designing and producing functional carbon materials for high-performance electrochemical devices.

Acknowledgements

This work was supported by the National Natural Science Foundation of China, the National High Technology Research and Development Program of China (863 Program, No. 2012AA053401 and 2013AA051002), the National Basic Research Program of China (973 Program, 2012CB215500 and 2012CB932800), and the Science & Technology Research Programs of Jilin Province (Nos. 20102204, 20100420).

References

[1] S. Wasmus, A. Küver, J. Electroanal. Chem. 461 (1999) 14–31.
[2] X. Zhao, M. Yin, L. Ma, L. Liang, C. Liu, J. Liao, T. Lu, W. Xing, Energy Environ. Sci. 4 (2011) 2736–2753.
[3] Y.-J. Wang, D.P. Wilkinson, J. Zhang, Chem. Rev. 111 (2011) 7625–7651.
[4] I. Mintsouli, J. Georgieva, S. Armyanov, E. Valova, G. Avdeev, A. Hubin, O. Steenhaut, J. Dille, D. Tsiplakides, S. Balomenou, S. Sotiropoulos, Appl. Catal. B: Environ. 136 (2013) 160–167.
[5] F. Su, Z. Tian, C.K. Poh, Z. Wang, S.H. Lim, Z. Liu, J. Lin, Chem. Mater. 22 (2009) 832–839.
[6] J. Qi, L.H. Jiang, S.L. Wang, G.Q. Sun, Appl. Catal. B: Environ. 107 (2011) 95–103.
[7] M. Rahsepar, M. Pakshir, P. Nikolaev, A. Safavi, K. Palanisamy, H. Kim, Appl. Catal. B: Environ. 127 (2012) 265–272.
[8] Y.K. Zhou, K. Neyerlin, T.S. Olson, S. Pylypenko, J. Bult, H.N. Dinh, T. Gennett, Z.P. Shao, R. O'Hayre, Energy Environ. Sci. 3 (2010) 1437–1446.
[9] Y.Y. Shao, J.H. Sui, G.P. Yin, Y.Z. Gao, Appl. Catal. B: Environ. 79 (2008) 89–99.
[10] J.R.C. Salgado, R.G. Duarte, L.M. Ilharco, A.M.B. do Rego, A.M. Ferraria, M.G.S. Ferreira, Appl. Catal. B: Environ. 102 (2011) 496–504.
[11] X. Zhao, J. Zhu, L. Liang, J. Liao, C. Liu, W. Xing, J. Mater. Chem. 22 (2012) 19718–19725.
[12] D.P. He, Y.L. Jiang, H.F. Lv, M. Pan, S.C. Mu, Appl. Catal. B: Environ. 132 (2013) 379–388.
[13] N.Y. Hsu, C.C. Chien, K.T. Jeng, Appl. Catal. B: Environ. 84 (2008) 196–203.
[14] Y.J. Hu, P. Wu, Y.J. Yin, H. Zhang, C.X. Cai, Appl. Catal. B: Environ. 111 (2012) 208–217.
[15] T. Maiyalagan, Appl. Catal. B: Environ. 80 (2008) 286–295.
[16] J.H. Kim, B. Fang, S.B. Yoon, J.S. Yu, Appl. Catal. B: Environ. 88 (2009) 368–375.
[17] Y. Wang, X. Wang, C.M. Li, Appl. Catal. B: Environ. 99 (2010) 229–234.
[18] Y. Ma, L. Sun, W. Huang, L. Zhang, J. Zhao, Q. Fan, W. Huang, J. Phys. Chem. C 115 (2011) 24592–24597.
[19] G. Wu, D. Li, C. Dai, D. Wang, N. Li, Langmuir 24 (2008) 3566–3575.
[20] B. Hu, K. Wang, L. Wu, S.-H. Yu, M. Antonietti, M.-M. Titirici, Adv. Mater. 9999 (2010) 813–828.
[21] L. Zhao, N. Baccile, S. Gross, Y. Zhang, W. Wei, Y. Sun, M. Antonietti, M.-M. Titirici, Carbon 48 (2010) 3778–3787.
[22] R. Demir Cakan, M.-M. Titirici, M. Antonietti, G. Cui, J. Maier, Y.-S. Hu, Chem. Commun. 44 (2008) 3759–3761.
[23] H.M. Yi, L.Q. Wu, W.E. Bentley, R. Ghodssi, G.W. Rubloff, J.N. Culver, G.F. Payne, Biomacromolecules 6 (2005) 2881–2894.
[24] H.-B. Yao, H.-Y. Fang, Z.-H. Tan, L.-H. Wu, S.-H. Yu, Angew. Chem. Int. Ed. 49 (2010) 2140–2145.
[25] S. Biniak, G. Szymański, J. Siedlewski, A. Świątkowski, Carbon 35 (1997) 1799–1810.
[26] Y. Chen, J. Wang, H. Liu, M.N. Banis, R. Li, X. Sun, T.-K. Sham, S. Ye, S. Knights, J. Phys. Chem. C 115 (2011) 3769–3776.
[27] R.J. Isaifan, S. Ntais, E.A. Baranova, Appl. Catal. A 464/465 (2013) 87–94.
[28] M. Arenz, K.J.J. Mayrhofer, V. Stamenkovic, B.B. Blizanac, T. Tomoyuki, P.N. Ross, N.M. Markovic, J. Am. Chem. Soc. 127 (2005) 6819–6829.
[29] T. Frelink, W. Visscher, J.A.R. van Veen, J. Electroanal. Chem. 382 (1995) 65–72.
[30] Y. Takasu, T. Iwazaki, W. Sugimoto, Y. Murakami, Electrochem. Commun. 2 (2000) 671–674.
[31] Z. Lei, M. Zhao, L. Dang, L. An, M. Lu, A.-Y. Lo, N. Yu, S.-B. Liu, J. Mater. Chem. 19 (2009) 5985–5995.
[32] B. Hammer, J.K. Norskov, Surf. Sci. 343 (1995) 211–220.
[33] B. Hammer, Top. Catal. 37 (2006) 3–16.